

Camphor-Based Closed-Cell Aluminium Foam Prepared by Powder Metallurgy Technique

Devendra PRASAD^a, Ajaya BHARTI^{a,1} and Naveen KUMAR^b

^a*Department of Applied Mechanics, Motilal Nehru National Institute of Technology
Allahabad, Prayagraj, 211004 India*

^b*Department of Mechatronics Engineering, Sanjivani College of Engineering,
Kopargaon, 423603 India*

Abstract. Metallic foams have attracted attention of all the industries because of their high strength to weight ratio and long life. Particularly, aluminium foams have approximately uniform pores in the structure which is responsible for their higher mechanical properties in comparison to the conventional structure. In the present work, the aluminium foams were developed by powder metallurgy technique using the camphor as a space holding and Al6061 powder as a matrix, mixed using a ball milling machine at 200 RPM for 30 minutes, compacted using a universal testing machine at 450 MPa pressure and sintered in a muffle furnace at 500°C for one hour, the camphor burns out and aluminium foam developed. With an increase in the volume fraction of camphor by volume up to 50%, porosity increases, compressive strength decreases by almost 66%, compressive strain increases by almost 100%, and the highest strain energy is absorbed by 30% camphor-based aluminium foam.

Keywords. Aluminium foam, metallic foam, closed cells, powder metallurgy, energy absorption

1. Introduction

Aluminium foam is lightweight material characterized by a combination of low density, higher porosity, higher energy absorbing properties, higher damping & acoustic dissipation properties, higher heat dissipation and good mechanical strength [1-6]. Because of its great mechanical and natural characteristics, it is preferred as lighter material for Aerospace, automobile, defence, military vehicles, and bullet trains for better fuel economy and higher energy absorption during a collision [7-9]. The metallic foam has two types one is open-cell which allows the fluid to penetrate and flow across it is mostly used for heat exchange and chemical circulation like as a bipolar plate of a PEM fuel cell [10]. Another is closed-cell having higher mechanical and energy-absorbing properties [11-13]. Because of these characteristics, closed-cell foam is used for structural components in Automotive, Locomotives, Construction and Building [14-15]. For the development of metallic foam using some different technology like Stir

¹ Ajaya BHARTI, Corresponding author, Department of Applied Mechanics, Motilal Nehru National Institute of Technology Allahabad, Prayagraj, 211004 India; E-mail: abharti@mnnit.ac.in.

casting, Lost foam casting, Injection of gas casting, Sintered fibre, Replication/ Space Holding technology, Additive manufacturing technology and Powder metallurgy technology [16-19]. During the production of metallic foam, many points need to consider like the cost of the production, material utilisation, thermal/electric power utilisation and easy production technology [20-21]. Also, some production technology created defects in physical characteristics, such as not uniform pores distribution, uneven pore size, misrun of materials, space holding materials floated out etc [22-23]. so overcome some problems using powder metallurgy for the development of aluminium foam, the density of materials can be reduced by adding the foaming agent in powder form which can be mixed properly and compact and sintered, foaming agent burnout and generates the pores in the structure which lowers the density hence reducing the mass of the structure [24-25].

In this present research work, a powder metallurgy technique was used to develop the aluminium foam by using camphor as a space holding, it shows more uniform pores in the structure.

2. Experiment

2.1. Materials

In the present research work, fine Aluminium alloys Al6061 powder having size 5-30 μm which is verified by figure 1 shows the SEM image of Al6061 powder used as a base material and camphor ($\text{C}_{10}\text{H}_{16}\text{O}$) powder as a space holding material its particle size 5-50 μm . Aluminium alloys having composition by weight fraction are Mg-0.8-1.2, Si- 0.40-0.80, Cu-0.15-0.40, Cr-0.04-0.35, Mn-0.15 max, Fe-0.70 max, Zn-0.15 max, Ti-0.25 max, Other are 0.05 max each and 0.15 max all and remaining are aluminium [26-27].

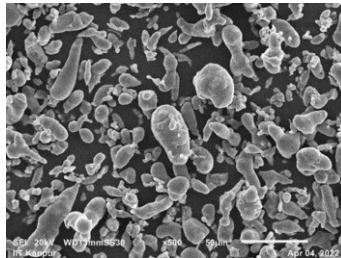


Figure 1. SEM of Aluminium powder.

2.2. Aluminium Foam Preparation

This research work used the powder metallurgy technique for the preparation of aluminium foam that contains Al6061 aluminium alloy powder at 30 μm particle size and camphor ($\text{C}_{10}\text{H}_{16}\text{O}$) powder (1-50 μm particle size) as a foaming agent. It is mixed in a ball milling machine at 200 rpm for 30 minutes, here power and steel ball ratio in the mass fraction is 1:4 [28]. To study the effect of porosity, four different fractions of camphor and aluminium by volume/volume- 20/80%, 30/70%, 40/60%, and 50/50% pure Al6061. The mixed powder of aluminium and camphor inserted in the die has a diameter of 20.20 mm. Then it was compacted by using a UTM machine (Model no-

ZD-40) at a pressure of 450 MPa, hence the green compact specimen was prepared [29-30]. After measuring the dimension and mass of the green compact, it is sintered in the closed Muffle furnace (Model no- AI-106) at a temperature of 500°C for one hour and the furnace is cooled to room temperature. During sintering camphor burn-out from the compact specimen generates pores, due to this process, aluminium foam is prepared [31-32]. Sample preparation and experimentation process is shown in figure 2.

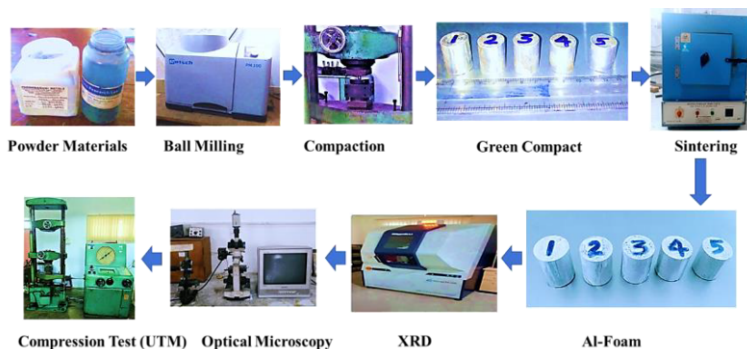


Figure 2. Sample preparation and experimentation process.

2.3. Characterization and Testing

To identify the different phases that are present in the crystalline sample, as well as to determine the size and strain, an X-ray diffraction study of the sample with a thickness of (3 mm) was performed. X-ray diffractograms are taken using an X-ray diffractometer which is installed in CIR lab MNNIT Allahabad.

The material's physical, mechanical, and other characteristics are influenced by the size of the grains, the presence of phases, and the interparticle adhesion. Therefore, optical microscopy is highly helpful for figuring out the differences in mechanical and other properties. Omnitech Optical microscopy is available in MS lab MNNIT Allahabad. An optical microscope uses visible light and a system of lenses to magnify images to observe the porosity of the aluminium foam.

Compression testing of samples was performed to know the compressive strength of the material. The compression test of the aluminium foam sample is prepared according to ISO 1314 standards. Small samples with a length-to-diameter ratio (L/D) of 0.8 were prepared. The compression test for different compositions was performed on a hydraulic Universal Testing Machine (UTM) [33-34].

3. Result and Discussion

The physical and mechanical properties of the aluminium foam are examined by the numerical and experimental techniques which are the following:

3.1. XRD of Aluminium Foam

The X-ray diffraction analysis image is shown in figure 3 which shows the different phases present in the aluminium foam. This XRD analysis observed that the phases of

Al, and AlMg, reveal the strengthening of metal foam and the oxide of aluminium like Al_2O_3 enhances the viscosity and reduction of intensity in terms of counts as per the porosity increases.

3.2. Scanning Electron Microscopy

Figure 4 shows the SEM image of aluminium foam pores distribution. For the development of aluminium foam after mixing the Al6061 powder and $C_{10}H_{16}O$ powder, compaction and sintering were done. During sintering, camphor burns out and creates the pores and agglomeration of aluminium particles in the sintered specimen which can be observed at the microscopy level by the SEM.

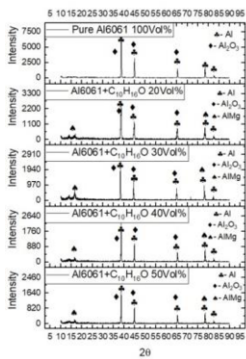


Figure 3. XRD of Aluminium Camphor based foam.

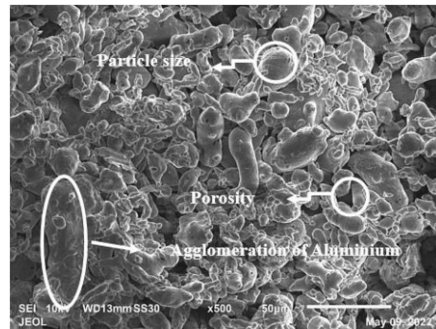


Figure 4. SEM of Sintered compact Aluminium foam.

3.3. Optical Microscopy

Figure 5 shows the optical microscopy of $C_{10}H_{16}O$ -based Aluminium foam. Here A denotes an optical microscopy image of the Pure Al6061 100Vol% and A' porosity. Similarly, B indicates Al6061+ $C_{10}H_{16}O$ 20Vol%, C- Al6061+ $C_{10}H_{16}O$ 30Vol%, D- Al6061+ $C_{10}H_{16}O$ 40Vol%, E- Al6061+ $C_{10}H_{16}O$ 50Vol% and A', B', C', D', & E' indicate the porosity in the green colour of the Al-foam which was measured by the Omnitech optical microscopy software as per the grey level available at pores. Porosity is more uniform at the particle size level and also at some position agglomeration of aluminium which reduces the porosity level.

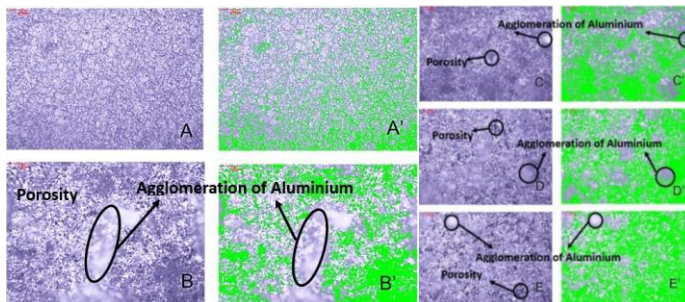


Figure 5. Optical microscopy of $C_{10}H_{16}O$ based Aluminium foam.

3.4. Density and Porosity Relation

After compaction by using a UTM machine the green compact specimen is produced by using the numerical formula technique (density is equal to mass divided by volume of the specimen), to find out the density and porosity deviation with a standard value. From the bar chart of the green compact aluminium foam which is shown in figure 6 for the pure Al-foam, the density is about 2.59 g/cm^3 and its porosity is about 3.997% only but camphor was added, the density of the green compact gradually decreases and porosity was increased. As per the volume fraction of camphor added at 20%, 30%, 40%, and 50% volume fraction of aluminium and camphor, the density reached the 2.338 g/cm^3 , 2.233 g/cm^3 , 2.078 g/cm^3 , and 1.979 g/cm^3 and porosity are 13.39%, 17.30%, 23.023%, and 26.261%.

After sintering the green specimen, the sintered compact specimen was produced. In the pure Al-foam, it was observed that sintering swollen specimen so the density is reduced and porosity is increased and Al-foam-camphor compacts during sintering and camphor burn out generates the pores in the specimen, hence foam is developed. With increasing the volume fraction of camphor 20%, 30%, 40%, 50% and pure aluminium the density of sintered compact is observed as 2.021 g/cm^3 , 1.798 g/cm^3 , 1.59 g/cm^3 , 1.34 g/cm^3 and 2.374 g/cm^3 and the percentage of porosity is observed as 25.128%, 33.385%, 41.092%, 50.344 and for pure aluminium 12.056%. Density and Porosity of the sintered compact specimen are shown in figure 7.

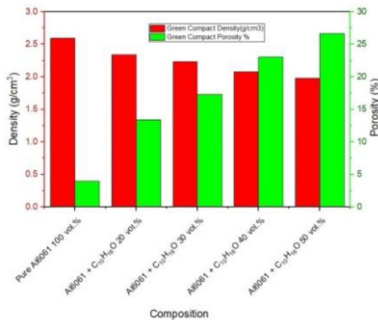


Figure 6. The Green Compact density and porosity.

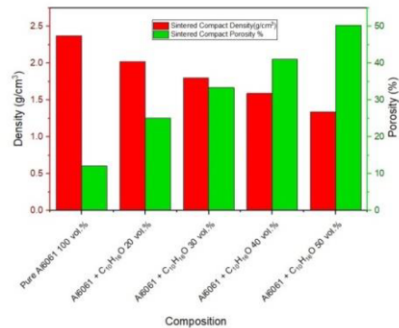


Figure 7. Density and Porosity of the sintered compact specimen.

3.5. Compression Test

The compression test performs on UTM machine model no- ZD40 at the strain rate of 0.01 to analyse the stress and strain behaviour of aluminium foam prepared using Al6061 & C₁₀H₁₆O at the volume fraction of 0%, 20%, 30%, 40%, and 50% of C₁₀H₁₆O by powder metallurgy technique shown in figure 8. The highest stress value obtained during the crushing of pure aluminium foam was 165.542 MPa, 20 Vol.% C₁₀H₁₆O aluminium foam 154.420 MPa, 30 Vol.% C₁₀H₁₆O Al-foam 135.738 MPa, 40 Vol.% C₁₀H₁₆O aluminium foam 104.560 MPa and 50 Vol.% C₁₀H₁₆O Al-foam 64.384 MPa at the percentage of strain are 40.117, 58.449, 67.980, 53.603 and 46.406. With an increase in the volume fraction of camphor by Volume up to 50%, porosity increases

and compressive strength decreased by almost 66%, and compressive strain increases by almost 100%.

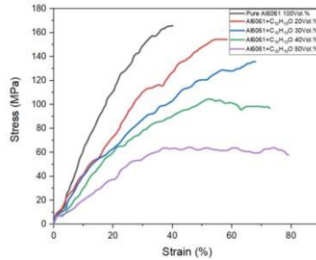


Figure 8. Stress-Strain curve of camphor-based closed cell Aluminium foam.

3.6. Compression Energy Absorption

After the compression test of different compositions of aluminium and camphor of aluminium foam, the stress-strain was obtained. The area occupied under the stress-strain curve is called toughness energy in the form of Jule. That is also known as the amount of strain energy absorbed by the samples during compression shown in figure 9. The highest amount of strain energy absorbs by the 30 Vol.% C₁₀H₁₆O aluminium foam is 59.5 Jule and for pure Al6061, 20%, 40%, and 50% volume fractions of camphor aluminium foam compression strain energy absorption are 41.5 Jule, 55.8 Jule, 54.1 Jule and 39.5 Jule.

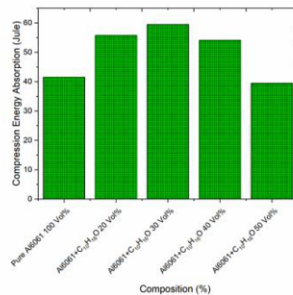


Figure 9. Compression Energy absorption of different composition of aluminium and camphor aluminium foam.

4. Conclusion

In the present work, aluminium foams have been successfully prepared using C₁₀H₁₆O by powder metallurgy techniques.

Due to high reactivity, aluminium reacted with oxygen to form alumina. XRD analysis confirmed the presence of Al₂O₃.

SEM analysis confirmed the formation of uniformly distributed close-cell porosity. In only a few places, the space holder didn't mix properly because the aluminium particle agglomerated and diffused together.

Optical microscopy also confirmed the formation of close cell porosity.

With an increase in the volume fraction of camphor, porosity is increased. The highest porosity 51.23% was obtained for the foam fabricated using 50% camphor.

With an increase in the volume fraction of camphor up to 50%, compressive strength is decreased by almost 66%.

With an increase in the volume fraction of camphor by 50%, compressive strain is increased by almost 100%.

The highest strain energy absorbing property was observed by the 30 Vol.% of camphor-based aluminium foam.

References

- [1] Kumar R, et al. Lightweight open-cell aluminium foam for superior mechanical and electromagnetic interference shielding properties. *Mater. Chem. Phys.* Jan. 2020; 240: 122-274.
- [2] Hanssen AG, Stöbener K, Rausch G, Langseth M and Keller H. Optimisation of energy absorption of an A-pillar by metal foam insert. *International Journal of Crashworthiness.* 2006; 11(3): 231-242.
- [3] Wang XF, Wei X, Han FS and Wang XL. Sound absorption of open-celled aluminium foam fabricated by investment casting method, *Materials Science and Technology*, 2011; 27(4): 800-804.
- [4] Baird KS and Williams JD. Density–energy relationships in explosive compaction of metal powders. *Powder Metallurgy.* 2022; 3(4): 281-285.
- [5] Bekoz N and Oktay E. High-temperature mechanical properties of low alloy steel foams produced by powder metallurgy. *Mater Des.* 2014; 53: 482-489.
- [6] Dvorák T and Kúdela S. Perforated closed-cell aluminium foam for acoustic absorption. *Applied Acoustics.* 2021; 174: 107706.
- [7] Ma CC, Lan FC, Chen JQ, Liu J and Zeng FB. Automobile crashworthiness improvement by energy-absorbing characterisation of aluminium foam porosity. *Materials Research Innovations.* 2015; 19: S1109-S1112.
- [8] Baird KS and Williams JD. Density–energy relationships in explosive compaction of metal powders. *Powder Metallurgy.* 2013; 30(4): 281-285.
- [9] Dineshkumar J, Jesudas T and Elayaraja R. Characteristics, applications and processing of aluminium foams – A review. *Mater. Today Proc.* 2021; 42(5): 1773-1776.
- [10] Liang L, Guo W, Zhang Y, Zhang W, Li L and Xing X. Radial basis function neural network for prediction of medium-frequency sound absorption coefficient of composite structure open-cell aluminium foam. *Applied Acoustics.* 2020; 170: 107505.
- [11] Hanssen AG, Lorenzi L, Berger KK, Hopperstad OS and Langseth M. A demonstrator bumper system based on aluminium foam filled crash boxes. *International Journal of Crashworthiness.* 2000; 5(4): 381-392.
- [12] Seitzberger M and Willminger S. Application of plastic collapse mechanisms for the axial crushing analysis of tubular steel structures filled with aluminium foam. *International Journal of Crashworthiness.* 2001; 6(2): 165-176.
- [13] Wang L, Zhang B, Zhang J, Jiang Y, Wang W and Wu G. Deformation and energy absorption properties of cenosphere-aluminium syntactic foam-filled tubes under axial compression. *Thin-Walled Structures,* Mar. 2021; 160: 107364.
- [14] Mandal DP, Majumdar DD, Bharti RK and Majumdar JD. Microstructural characterisation and property evaluation of titanium cenosphere syntactic foam developed by powder metallurgy route. *Powder Metallurgy.* Sep. 2015; 58(4): 289-299.
- [15] Li Y, Lv Z and Wang Y. Blast response of aluminium foam sandwich panel with double V-shaped face plate. *Int. J. Impact. Eng.* Nov. 2019; 144: 103666.
- [16] Vogiatzis CA, Tsouknidas A, Kountouras DT and Skolianos S. Aluminum–ceramic cenospheres syntactic foams produced by powder metallurgy route. *Mater. Des.* Nov. 2015; 85: 444-454.
- [17] Gruttadauria A, Barella S, Mapelli C, Mombelli D and Castrodeza EM. Production of 17CrMoV5-11 steel sponges utilising powder metallurgical replication technique with SiC as a space holder. *Powder Metallurgy.* 2016; 59(2): 95-99.
- [18] Hashim UR, Jumahat A, Ismail MH and Razali RNM. Fabrication and characterisation of carbon fibre reinforced polymer rods with an aluminium foam core. *Materials Research Innovations.* Dec. 2014; 18: S6-204-S6-208.

- [19] Mustapha M, Mustapha F, Mamat O and Hussain P. Fabrication of aluminium foam through pressure assisted high-frequency induction heated sintering dissolution process: An experimental observation. *Powder Metallurgy*. Jul. 2011; 54(3): 343-353.
- [20] Ding X, Liu Y, Chen X, Zhang H and Li Y. Optimization of the cellular structure of aluminium foams produced by powder metallurgy method. *Mater. Lett. Apr.* 2018; 216: 38-41.
- [21] Li A, Xu HY, Geng L, Li BL, Tan ZB and Ren W. Preparation and characterization of SiCp/2024Al composite foams by powder metallurgy. *Transactions of Nonferrous Metals Society of China*. Oct. 2012; 22: s33-s38.
- [22] Zhang P, Haag M, Kraft O, Wanner A and Arzt E. Microstructural changes in the cell walls of a closed-cell aluminium foam during creep. 2009; 82,(16): 2895-2907.
- [23] Ha W, Kim SK, Jo HH and Kim YJ. Optimisation of process variables for manufacturing aluminium foam materials using aluminium scrap. *Materials Science and Technology*. 2005; 21(4): 495-499.
- [24] Velasco B, Tsipas SA, Ferrari B and Gordo E. MAX phase foams produced via powder metallurgy process using water-soluble space holder. *Powder Metallurgy*. Apr. 2015; 58(2): 95-99.
- [25] Vogiatzis CA and Skolianos SM. On the sintering mechanisms and microstructure of aluminium-ceramic cenospheres syntactic foams produced by powder metallurgy route. *Compos. Part A Appl. Sci. Manuf.* Mar. 2016; 82: 8-19.
- [26] Asghar Z, et al. Effect of distribution of B4C on the mechanical behaviour of Al-6061/B4C composite. *Powder Metallurgy*. Aug. 2018; 61(4): 293-300.
- [27] Wang L, Hua ZS, Ma J and Yao GC. Effects of Mg addition on foam stability of Al foams made by powder metallurgy route. *Powder Metallurgy*. Jul. 2011; 54(3):385-388.
- [28] Ditenberg IA, Osipov DA, Korchagin MA, Smirnov IV, Grinyaev KV and Gavrilov AI. Influence of ball milling duration on the morphology, features of the structural-phase state and microhardness of 3Ni-Al powder mixture. *Advanced Powder Technology*, 2021; 32(10): 3447-3455.
- [29] Kumar N, Bharti A, and Devendra P. An analysis on the techniques of iron and steel metallic foams fabrication. *Powder Metallurgy and Metal Ceramics*, 2022.
- [30] Kumar N and Bharti A. Review on powder metallurgy: a novel technique for recycling and foaming of aluminium-based materials. *Powder Metallurgy and Metal Ceramics*. 2021; 60(01): 52-59.
- [31] Gülsoy HÖ and German RM. Sintered foams from precipitation hardened stainless steel powder. *Powder Metallurgy*. 2008; 51(4): 350-353.
- [32] Mustapha M, Mustapha F, Mamat O and Hussain P. Fabrication of aluminium foam through pressure assisted high-frequency induction heated sintering dissolution process: An experimental observation. *Powder Metallurgy*. Jul. 2011; 54(3):343-353.
- [33] Castro G, Nutt SR and Wenchen X. Compression and low-velocity impact behaviour of aluminium syntactic foam. *Materials Science and Engineering: A*. Aug. 2013; 578: 222-229.
- [34] Kriszt B, Foroughi B, Faure K and Degischer HP. Behaviour of aluminium foam under uniaxial compression. *Materials Science and Technology*. 2000; 16(7-8): 792-796.